

Supplementary Information for

**A Chemical Dynamics Study on the Gas Phase Formation of
Thioformaldehyde (H₂CS) and its Thiohydroxycarbene
Isomer (HCSH)**

Srinivas Doddipatla, Chao He, Ralf I. Kaiser*

Department of Chemistry, University of Hawai‘i at Mānoa, Honolulu, HI 96822

Yuheng Luo, Rui Sun*

Department of Chemistry, University of Hawai‘i at Mānoa, Honolulu, HI 96822

Galiya R. Galimova, Alexander M. Mebel*

Department of Chemistry and Biochemistry, Florida International University, Miami, FL, 33199

Tom J. Millar*

*School of Mathematics and Physics, Astrophysics Research Centre, Queen’s University Belfast,
Northern Ireland, UK, BT7 1NN*

*Correspondence to: ralfk@hawaii.edu, ruisun@hawaii.edu, mebela@fiu.edu, Tom.Millar@qub.ac.uk

Identification of the Electronic Structure Method for Quasi-classical Trajectory (QCT)

Simulation. The quantum chemistry method employed for QCT simulations needs to accurately represent the potential energy of this reaction and to be computationally efficient (1). Therefore, the potential energy profile from a series of combinations of single reference method (i.e. MP2 (2) and DFTs (3)) and double-zeta basis sets are compared against the benchmark values (Figure 4), which are generated from CCSD(T)-F12 (4) /cc-pVQZ-f12 (5) //B2PLYPD3 (6) /cc-pVTZ (7). Three well-adapted criteria (8-10) are applied in selecting an optimal method for the QCT simulations: #1. the method must be able to locate all the reactants, products, transition states, and intermediates; #2. the method must be stable in the QCT simulations, which mostly are sampling non-optimized structure; and finally, #3. for those methods that satisfy #1 and #2, their corresponding potential energy profile should be as close to the benchmark as possible. To quantify #3, the root mean square displacement (RMSD) between the benchmark value and the candidate method is computed with the following equation:

$$RMSD = \sqrt{\frac{1}{N} \sum_{i=1}^N \delta_i^2}, \quad \delta_i = PE(i) - PE_{ref}(i) \quad [S1]$$

in which δ_i is the difference in relative potential energy between the benchmark value and the value from the candidate method, and N is the total number of points on the potential energy profile that are characterized, including the reactants, products, transition states, and intermediates. The results are summarized in Table S1. Though Becke97 (11) /aug-cc-pVDZ (7) and M06 (12) /6-311++G** (13) have the minimal RMSD values, the total energy of the QCT simulations is not stable (violating #2), and hence B3LYP (14) /aug-cc-pVDZ (7) is selected.

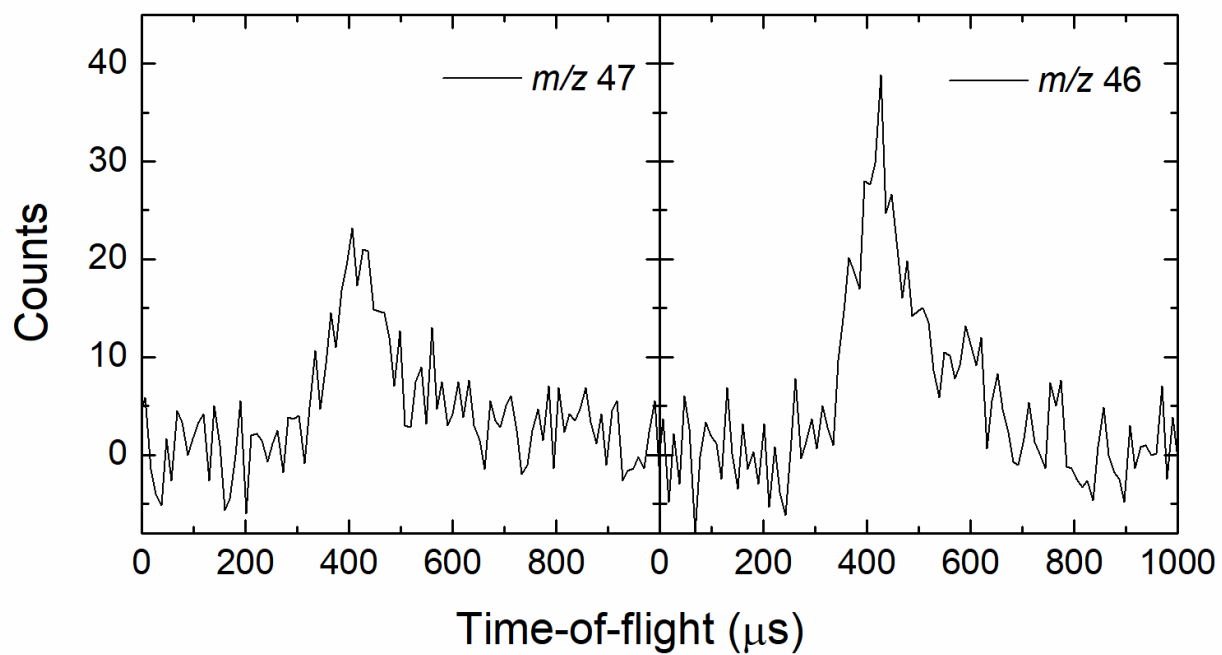


Fig S1. Time-of-flight spectra for the reaction of D1-methylidyne radical (CD) with hydrogen sulfide (H_2S).

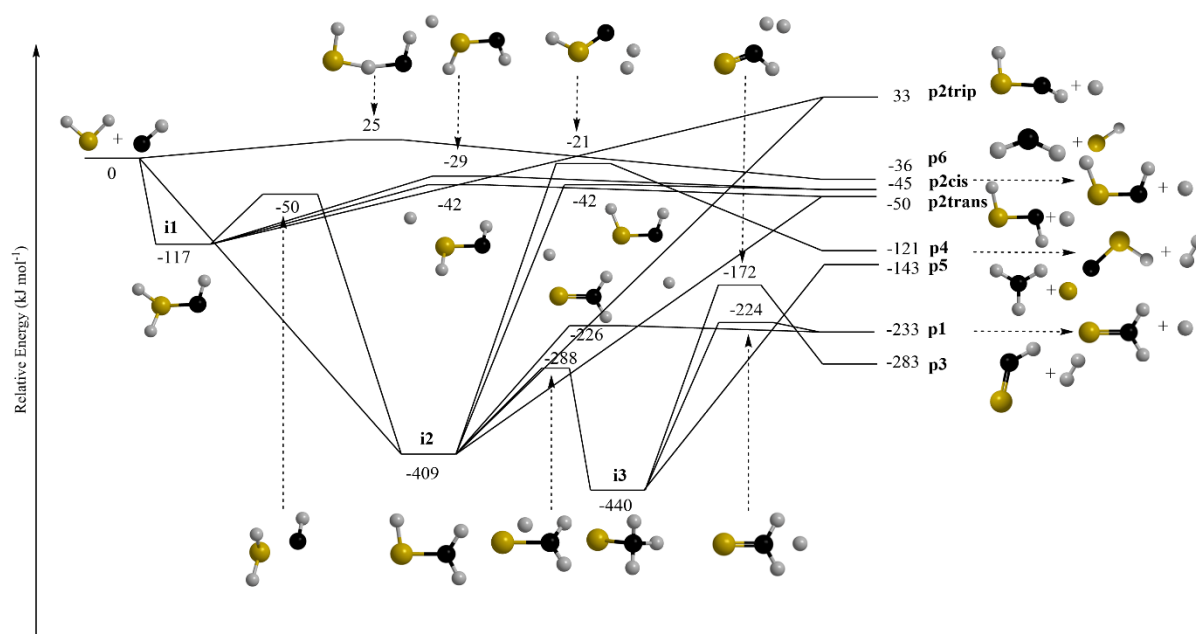


Fig. S2. Potential energy surface for the reactions of hydrogen sulfide (H₂S) with methylidyne radical (CH). Relative energies calculated at the CCSD(T)-F12/cc-pVQZ-f12//B2PLYPD3/cc-pVTZ + ZPE(B2PLYPD3/cc-pVTZ) level of theory are given in units of kJ mol⁻¹. Colors of the atoms: sulfur (yellow), carbon (black), and hydrogen (gray).

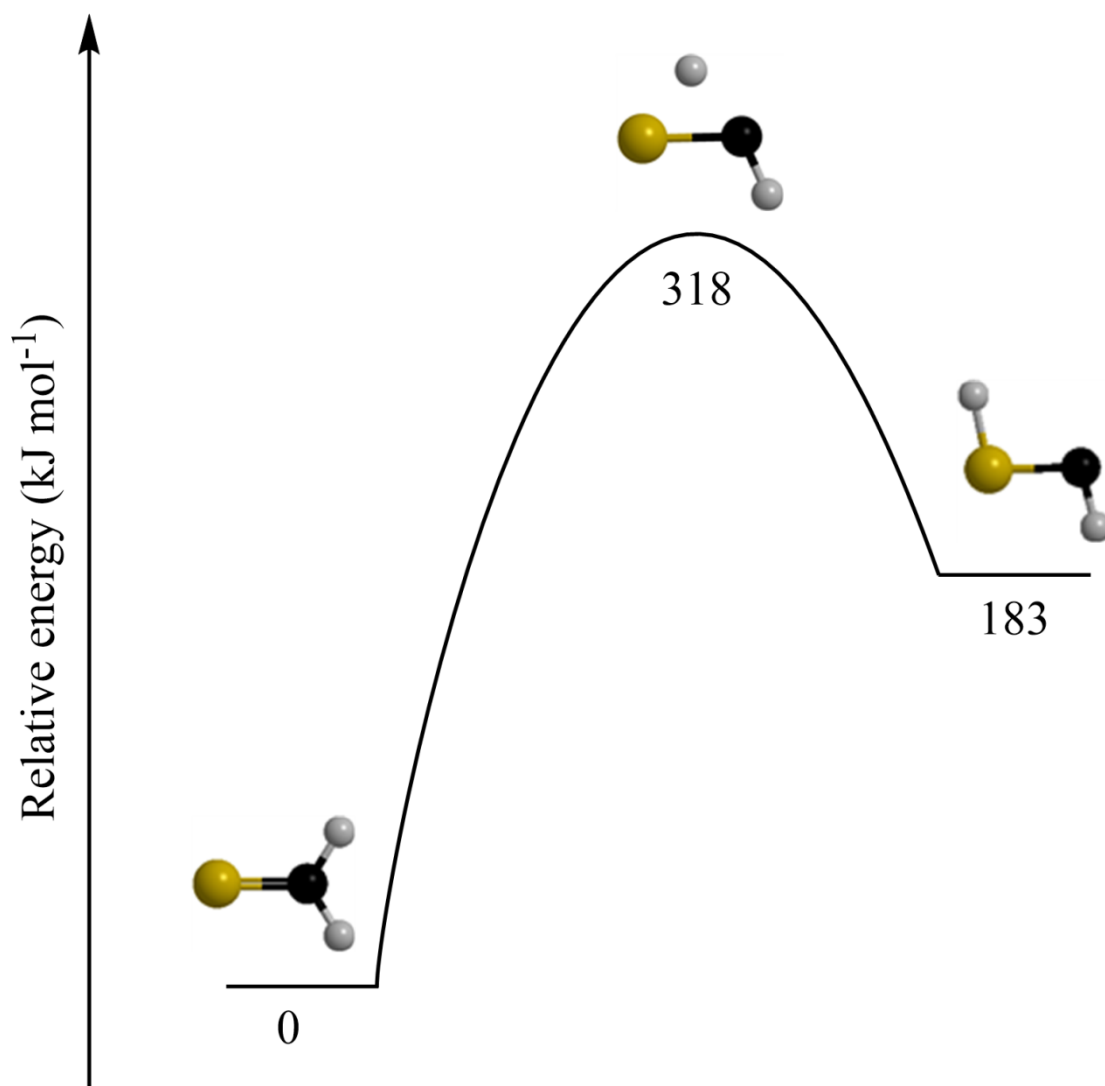


Fig. S3. Isomerization of thiohydroxycarbene into thioformaldehyde calculated at the CCSD(T)-F12/cc-pVQZ-f12//B2PLYPD3/cc-pVTZ + ZPE(B2PLYPD3/cc-pVTZ) level of theory. Colors of the atoms: sulfur (yellow), carbon (black), and hydrogen (gray).

Table S1. Peak velocities (v_p) and speed ratios (S) of methylidyne radical (CH; $X^2\Pi$), D1-methylidyne radical (CD; $X^2\Pi$), hydrogen sulfide (H₂S; X^1A_1) and deuterium sulfide (D₂S; X^1A_1) beams along with the collision energy (E_C) and center-of-mass angle (Θ_{CM}).

beam	v_p (m s ⁻¹)	S	E_C (kJ mol ⁻¹)	Θ_{CM} (deg)
CH ($X^2\Pi$)	1834 ± 25	10.7 ± 1.3		
H ₂ S (X^1A_1)	805 ± 9	12.4 ± 0.1	18.9 ± 0.4	48.9 ± 0.4
D ₂ S (X^1A_1)	801 ± 21	12.8 ± 0.8	19.1 ± 0.4	50.4 ± 0.8
CD ($X^2\Pi$)	1849 ± 8	11.3 ± 2.1		
H ₂ S (X^1A_1)	805 ± 9	12.4 ± 0.1	20.1 ± 0.2	46.6 ± 0.7

Table S2. The RMSD of each electronic structure method with respect to the benchmark value (CCSD(T)-F12/cc-pVQZ-f12//B2PLYPD3/cc-pVTZ) are summarized in the table. The units of energy are kJ mol⁻¹. N/A indicates at least one of the configurations on the potential energy profile (Fig. 4) is not found with the corresponding electronic structure method.

Basis Set	Method					
	MP2	B3LYP	M05	M06	BECKE97	BECKE98
aug-cc-pVDZ	14	9	9	N/A	N/A	N/A
cc-pVDZ	22	N/A	9	N/A	6	N/A
6-31+G*	N/A	N/A	14	12	N/A	N/A
6-311++G**	N/A	N/A	9	6	N/A	N/A

Table S3. Number of detected trajectories for each pathway from the QCT simulations. 100 trajectories are sampled at each impact parameter. The last column is the overall ratio of each pathway after properly weighting the results from different impact parameters.

	Impact Parameter (Angstrom)					
	1.0	2.0	3.0	4.0	5.0	Overall (%)
Non-reactive	50	44	52	84	100	63 ± 2
Reactive	50	56	48	16	0	37 ± 2
(P1) SCH ₂ + H	26	28	26	10	0	20 ± 1
(P2) HSCH (cis/trans) + H	12	19	12	0	0	8 ± 1
(P3) CSH + H ₂	0	0	0	0	0	0
(P4) SCH + H ₂	9	3	4	0	0	3 ± 1
(P5) CH ₃ + S	0	0	0	0	0	0
(P6) CH ₂ + SH	3	6	6	6	0	6 ± 2

Table S4. Number of addition (forming i1) and insertion (forming i2) hydrogen atom emitting trajectories. 100 trajectories are sampled at each impact parameter. The last column is the overall ratio after properly weighting the results from different impact parameters.

	Impact Parameter (Angstrom)					
	1.0	2.0	3.0	4.0	5.0	Overall (%)
Addition (forming i1)	23	32	24	5	0	63 \pm 3
Insertion (forming i2)	15	15	14	5	0	37 \pm 3

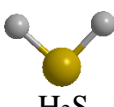
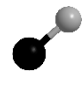
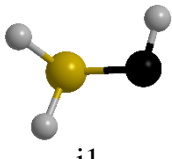
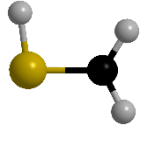
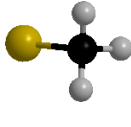
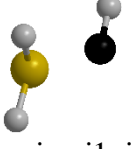
Table S5. Number of hydrogen atom emitting trajectories. The proton initially belonging to methylidyne radical is denoted in light blue. 100 trajectories are sampled at each impact parameter. The last column is the branching ratio after properly weighting the results from different impact parameters.

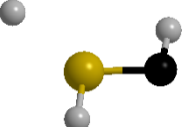
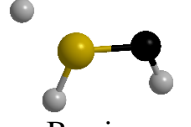
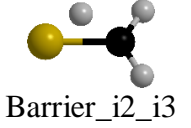
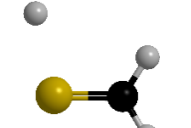
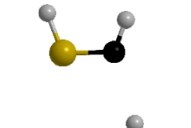

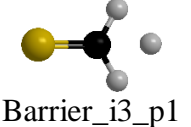
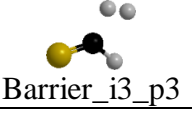
	Impact Parameter (Angstrom)					
	1.0	2.0	3.0	4.0	5.0	Overall (%)
(P1) SCHH + H	8	5	5	2	0	14 ± 2
(P1) SCH H + H	18	23	21	8	0	56 ± 3
(P2) H SCH (cis) + H	0	0	0	0	0	0
(P2) HSCH (cis) + H	4	5	1	0	0	6 ± 1
(P2) HSCH (cis) + H	0	0	0	0	0	0
(P2) H SCH (trans) + H	0	0	0	0	0	0
(P2) HSCH (trans) + H	8	14	11	0	0	24 ± 3
(P2) HSCH (trans) + H	0	0	0	0	0	0

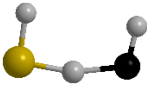
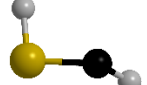
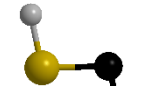
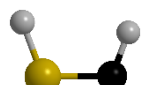
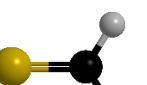
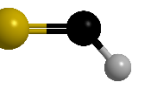

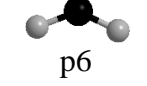
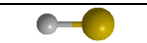
Table S6. Statistical product branching ratios computed using RRKM theory at the collision energy of 19 kJ mol⁻¹.

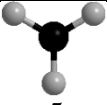
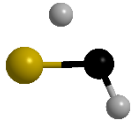
	from i1	from i2	63% i1 /37% i2
p1	48.77%	95.97%	66.23%
p2trans	43.63%	0.51%	27.67%
p2cis	6.69%	0.36%	4.35%
p3	0.77%	2.65%	1.47%
p4	0.00%	0.00%	0.00%
p5	0.15%	0.51%	0.28%

Table S7. Optimized Cartesian coordinates (Å), and vibrational frequencies(cm^{-1}) of reactants, intermediates, transition states, and dissociation products involved in the hydrogen sulfide (H_2S) + methyldiyne radical (CH)reaction.

Species	Vibrational Frequencies (cm^{-1})	Cartesian Coordinates (Å)			
		Atom	X	Y	Z
 H_2S	1215.2375, 2727.2450, 2745.4050	S H H	0.000000 0.968010 -0.968010	0.102920 -0.822394 -0.824333	0.000000 0.000000 0.000000
 CH	2874.2908	C H	0.000000 0.000000	0.000000 0.000000	0.159796 -0.958776
 $i1$	449.2044, 591.7365, 675.4046, 797.2839, 1104.9172, 1252.0658, 2250.1883, 2648.4517, 3031.9769	S C H H H	-0.446904 1.261716 -1.159076 -0.931732 1.670979	0.029149 -0.170172 0.810066 -1.099775 0.844363	-0.106332 0.082220 0.795418 0.441925 -0.029350
 $i2$	66.9577, 340.7753, 788.1840, 852.1739, 1079.2202, 1424.6806, 2721.2232, 3204.7371, 3335.5884	S C H H H	0.580993 -1.137239 0.850140 -1.640020 -1.682579	-0.088682 0.021661 1.223846 0.969589 -0.904494	-0.002180 0.009377 0.019653 -0.034937 -0.006092
 $i3$	586.4767, 724.5610, 873.3026, 1344.2948, 1396.0499, 1487.2945, 3043.7637, 3120.0914, 3141.2921	C S H H H	1.108097 -0.692158 1.503291 1.418646 1.504012	0.000221 0.000003 0.902021 -0.014844 -0.888547	0.008066 0.001968 0.467070 -1.038464 0.491513
 Barrier_{i1_i2} (-50)	964.4906i, 335.5239, 498.3836, 671.5021, 1100.5671, 1151.3687, 2373.1620, 2691.6492, 2878.1794	S C H H H	-0.582897 1.414190 0.137341 -0.915824 1.619702	0.095771 -0.195731 -0.052648 -1.205159 0.899864	-0.040419 -0.062737 1.130226 -0.068475 -0.038630

 Barrier_i1_p2trans	344.2012i, 250.0558, 935.2848, 1151.9207, 3011.1978	125.1382, 870.5178, 984.1950, 2603.6825,	S C H H H	-0.374532 1.237853 -2.267402 -0.766839 1.599634	-0.052889 -0.004843 1.124048 -1.126417 0.877652	-0.147141 0.229929 0.721339 0.574331 -0.320989
 Barrier_i1_p2cis	612.0408i, 400.4711, 925.7375, 1170.6397, 3068.5500	232.1297, 781.5210, 974.6004, 2424.7966,	S C H H H	0.401122 -1.215257 0.830353 1.677533 -1.634291	-0.125760 0.177806 -0.563528 1.521046 -0.012190	-0.111979 -0.094437 1.119177 0.339947 0.899164
 Barrier_i2_i3	1602.4107i, 640.2931, 937.1275, 2179.9877, 3285.0810	461.8339, 789.4789, 1419.2658, 3153.1361,	S C H H H	0.648095 -1.136986 -0.215270 -1.666188 -1.666149	-0.000167 -0.000199 0.004685 -0.937367 0.936558	-0.040197 -0.042297 1.118420 -0.107815 -0.113672
 Barrier_i2_p1	374.9387i, 304.2746, 1033.9041, 1506.5608, 3187.0363	138.9298, 1001.3779, 1176.0360, 3098.0045,	S C H H H	0.518874 -1.062692 -1.770346 -1.479743 1.324263	-0.187785 0.101349 -0.629051 1.039587 1.985923	-0.020609 0.004088 0.382458 -0.348262 0.271021
 Barrier_i2_p2cis	167.8421i, 68.0455, 973.2128, 1164.2430, 3069.8123	49.4510, 797.9883, 980.1721, 2406.5901,	S C H H H	-0.510067 0.984857 -1.414140 0.972711 2.693362	-0.199571 0.453578 0.731299 1.496830 -1.756462	-0.023894 -0.095050 0.436159 0.236849 0.279600
 Barrier_i2_p4	1004.0859i, 469.6863, 682.5890, 1178.3109, 2921.7399	378.9997, 605.4788, 899.7904, 677.7853,	S C H H H	0.568862 -1.087749 1.043735 -1.725823 -1.893206	-0.123377 0.446199 0.979592 -1.034490 -0.648259	-0.037220 -0.060124 0.566474 0.555987 -0.166200
 Barrier_i3_p1	607.9580i, 360.3149, 1041.1434, 1503.1728, 3175.7638	258.6768, 1011.2774, 1094.8162, 3090.3179,	C S H H H	-0.925367 0.656632 -1.989843 -1.482034 -1.482036	-0.268213 0.050529 1.640753 -0.419975 -0.419956	-0.000001 0.000000 0.000008 0.919742 -0.919746
 Barrier_i3_p3	1249.6833i, 756.5137, 1021.8604,	489.1612, 835.7579, 1090.4642,	S C H	-0.667946 0.915293 1.525516	0.040796 -0.234414 -1.000110	0.014524 -0.109461 0.350148

	1447.5493, 3188.1180	2468.6314,	H 1.939287 1.024598 0.449016 H 1.730570 0.729259 -0.374777
 Barrier_p0_p6	857.3860i, 328.1657, 711.7763, 1236.4769, 2926.6902	274.0107, 678.2821, 896.6363, 2722.4515,	C -2.030492 -0.150485 -0.000072 H -2.128286 0.958519 0.000697 S 0.885789 -0.062697 0.000056 H 0.717577 1.267862 -0.000659 H -0.578969 -0.320314 -0.000495
 p2trip	439.7003, 898.0006, 2580.9319,	830.3309, 932.8975, 3188.3082	S 0.506937 -0.092119 0.012922 C -1.168579 0.046835 -0.145403 H 0.845689 1.216813 0.061112 H -1.945214 -0.023912 0.604551
 p2trans	877.0186, 989.0554, 2596.3704,	954.2398, 1183.6469, 2997.8125	S 0.472497 -0.107460 0.000008 C -1.154580 0.225138 0.000029 H 0.971824 1.150287 -0.000138 H -1.604295 -0.781749 -0.000171
 p2cis	791.1719, 960.2953, 2416.6601,	946.4897, 115.8885, 3067.8387	S 0.477708 -0.082370 0.000009 C -1.161181 -0.130744 -0.000029 H 0.908263 1.223506 -0.000095 H -1.584502 0.878881 0.000120
 p1	1010.1859, 1081.5613, 3089.4525,	1029.3563, 1502.5451, 3176.7164	S -0.585774 0.000047 -0.000026 C 1.027717 0.000100 0.000267 H 1.601959 -0.921550 -0.000590 H 1.604119 0.920198 -0.000591
 p3	839.7305, 3131.0735	1207.1527,	S 0.035395 -0.507747 0.000000 C 0.035395 1.057725 0.000000 H -0.778682 1.777606 0.000000
 p4	784.6092, 2416.6202	929.5899,	S 0.058014 -0.417397 0.000000 C 0.058014 1.234396 0.000000 H -1.276309 -0.728028 0.000000
 p6	1092.5472, 3393.6600	3157.1527,	C 0.000000 0.104627 0.000000 H 0.990437 -0.313881 0.000000 H -0.990437 -0.313881 0.000000
 SH	2708.0083		S 0.000000 0.000000 0.079090 H 0.000000 0.000000 -1.265435

 <p>p5</p>	514.9536, 1427.6776, 1427.7996, 3139.6088, 3320.8118, 3321.0012	C -0.000005 0.000012 0.000179 H -1.011657 0.366022 -0.000358 H 0.822864 0.693042 -0.000358 H 0.188824 -1.059137 -0.000358
 <p>Barrier_ p1_p2trans</p>	1818.8697 <i>i</i> 516.0365 827.8811 1094.7729 2209.9939 2989.4852	S 0.551220 -0.057660 0.000000 C -1.156872 0.101752 0.000000 H -1.677225 -0.865452 0.000000 H -0.201054 1.177497 0.000000

Representative trajectories from QCT simulations. The proton initially belonging to methylidyne radical is colored in light blue to highlight the possible proton transfer. The following trajectories are visualized via movies:

Movie S1. **i1 \rightarrow i2 \rightarrow p1 + H** (top panel of Fig. 5)

Movie S2. **i2 \rightarrow i3 \rightarrow i2 \rightarrow p1 + H**

Movie S3. **i2 \rightarrow p1 + H**

Movie S4. **i1 \rightarrow (cis-)p2 + H**

Movie S5. **i1 \rightarrow (trans-)p2 + H** (bottom panel of Fig. 5)

Movie S6. **i1 \rightarrow i2 \rightarrow i3 \rightarrow p4**

Movie S7. **i1 \rightarrow i2 \rightarrow p6**

References

- (1) S. Pratihari, X. Ma, Z. Homayoon, G. L. Barnes, W. L. Hase, Direct Chemical Dynamics Simulations. *J. Am. Chem. Soc.* **139**, 3570–3590, (2017).
- (2) C. Möller, M. S. Plesset, Note on an Approximation Treatment for Many-Electron Systems. *Phys. Rev.* **46**, 618–622, (1934).
- (3) R. G. Parr, Density Functional Theory of Atoms and Molecules. In *Horizons of Quantum Chemistry*; K. Fukui, B. Pullman, Eds.; Springer Netherlands: Dordrecht, 5–15, (1980)
- (4) T. B. Adler, G. Knizia, H. J. Werner, A Simple and Efficient CCSD(T)-F12 Approximation. *J. Chem. Phys.* **22**, 127, (2007).
- (5) K. A. Peterson, T. B. Adler, H. J. Werner, Systematically Convergent Basis Sets for Explicitly Correlated Wavefunctions: The Atoms H, He, B-Ne, and Al-Ar. *J. Chem. Phys.* **8**, 128, (2008).
- (6) S. Grimme, Semiempirical Hybrid Density Functional with Perturbative Second-Order Correlation. *J. Chem. Phys.* **3**, 124 (2006).
- (7) T. H. Dunning, Gaussian Basis Sets for Use in Correlated Molecular Calculations. I. The Atoms Boron through Neon and Hydrogen. *J. Chem. Phys.* **90**, 1007–1023, (1989).
- (8) A. Shoji, D. Schanzenbach, R. Merrill, J. Zhang, L. Yang, R. Sun, Theoretical Study of the Potential Energy Profile of the $\text{HBr}^+ + \text{CO}_2 \rightarrow \text{HOCO}^+ + \text{Br}^\cdot$ Reaction. *J. Phys. Chem. A.* **123**, 9791–9799, (2019).
- (9) R. Sun, C. J. Davda, J. Zhang, W. L. Hase, Comparison of Direct Dynamics Simulations with Different Electronic Structure Methods. $\text{F}^- + \text{CH}_3\text{I}$ with MP2 and DFT/B97-1. *Phys. Chem. Chem. Phys.* **17**, 2589–2597, (2015).
- (10) J. Zhang, U. Lourderaj, S. V. Addepalli, W. a de Jong, W. L. Hase, Quantum Chemical Calculations of the $\text{Cl}^- + \text{CH}_3\text{I} \rightarrow \text{CH}_3\text{Cl} + \text{I}^-$ Potential Energy Surface [†]. *J. Phys. Chem. A.* **113**, 1976–1984, (2009).
- (11) A. D. Becke, Density-Functional Thermochemistry. V. Systematic Optimization of

- Exchange-Correlation Functionals. *J. Chem. Phys.*, **107**, 8554–8560, (1997).
- (12) Y. Zhao, D. G. Truhlar, A New Local Density Functional for Main-Group Thermochemistry, Transition Metal Bonding, Thermochemical Kinetics, and Noncovalent Interactions. *J. Chem. Phys.* **125**, 19, (2006).
- (13) R. Krishnan, J. S. Binkley, R. Seeger, J. A. Pople, Self-Consistent Molecular Orbital Methods. XX. A Basis Set for Correlated Wave Functions. *J. Chem. Phys.* **72**, 650–654. (1980).
- (14) A. D. Becke, Density-Functional Thermochemistry. III. The Role of Exact Exchange. *J. Chem. Phys.* **98**, 5648–5652, (1993).